



1 Future interannual variability of Arctic sea ice in coupled
2 climate models

3
4 John R. Mioduszewski¹, Stephen Vavrus¹, Muyin Wang^{2,4}, Marika Holland³, and Laura
5 Landrum³
6

7
8 ¹Nelson Institute Center for Climatic Research, University of Wisconsin—Madison, Madison,
9 Wisconsin.

10 ²Joint Institute for the Study of the Atmosphere and Oceans, University of Washington, Seattle,
11 Washington.

12 ³National Center for Atmospheric Research, Boulder, Colorado.

13 ⁴Pacific Marine Environmental Laboratory, National Oceanic and Atmospheric Administration,
14 Seattle, Washington.

15

16

17

18

19

20

21

22

23

24

25

26

27

28

29

30

31

32

33

34

35

36

37

38

39

40

41

42

43

Corresponding author: Steve Vavrus, svavrus@wisc.edu



44 Abstract

45

46 The diminishing Arctic sea ice pack has been widely studied, but mostly focused on time-mean
47 changes in sea ice rather than on short-term variations that also have important physical and soci-
48 etal consequences. In this study we test the hypothesis that future interannual Arctic sea ice area
49 variability will increase by utilizing a set of 40 independent simulations from the Community
50 Earth System Model's Large Ensemble (CESM-LE) for the 1920-2100 period, and augment this
51 with simulations from 12 models participating in the Coupled Model Intercomparison Project
52 Phase 5 (CMIP5). Both CESM-LE and CMIP5 models project that ice area variability will in-
53 deed grow substantially, but not monotonically, in all months, and with a strong seasonal de-
54 pendence in magnitude and timing that is robust among CESM ensemble members. The variabil-
55 ity in every month is inversely correlated with the average ice retreat rate before there is an even-
56 tual disappearance in both terms as the ice pack becomes seasonal in summer and autumn by late
57 century. The peak in variability correlates best with the total area of ice between 0.2 m and 0.6 m
58 monthly thickness, indicating that substantial future thinning of the ice pack is required before
59 variability maximizes. Within this range, the most favorable thickness for high areal variability
60 depends on the season, primarily due to whether ice growth or ice retreat processes dominate.
61 Thermodynamic processes are found to be more important than dynamical mechanisms, namely
62 ice export and ridging, in controlling ice area variability.

63

64

65

66

67

68

69

70

71

72

73

74

75

76

77

78

79

80

81

82

83

84

85

86

87

88

89



90 1. Introduction

91
92 Arctic sea ice extent has declined by more than 40% since 1979 during summer (e.g.
93 Stroeve et al. 2012; Serreze and Stroeve 2015; Comiso et al. 2017), primarily as a consequence
94 of greenhouse gas forcing (Notz and Marotzke 2012) but also internal variability (Ding et al.
95 2017). While this trend is greatest in summer, substantial losses are observed throughout the year
96 (Cavalieri and Parkinson 2012) resulting in an ice season duration that is up to 3 months shorter
97 in some regions (Stammerjohn et al. 2012). Reduced ice area is accompanied by a greater frac-
98 tion of younger ice (Nghiem et al. 2006; Maslanik et al. 2007a, 2011), which reduces the thick-
99 ness of the mean basin ice pack (Kwok and Rothrock 2009; Kwok et al. 2009; Lang et al. 2017).
100 As a result, the negative trend in sea ice volume (-27.9% per decade) is about twice as large as
101 the trend in sea ice area (-14.2% per decade; Overland and Wang 2013).
102

103 Many climate models suggest that the Arctic sea ice cover will not retreat in a steady
104 manner, but will likely fluctuate more as it diminishes, punctuated by occasional Rapid Ice Loss
105 Events (RILEs; Holland et al. 2006; Döscher and Koenigk 2013). The overall decline in ice
106 cover is expected to continue (Collins et al. 2013), and the Arctic will likely become seasonally
107 ice-free within a few decades, depending on emissions pathway (Stroeve et al. 2007; Wang and
108 Overland 2009; 2012; Massonet et al. 2012; Wang and Overland 2012; Overland and Wang
109 2013; Jahn et al. 2016; Notz and Stroeve 2016). However, internal variability confounds predic-
110 tion of this timing (Stocker et al. 2013; Swart et al. 2015; Jahn et al. 2016; Labe et al. 2018), and
111 even the definition of ice-free differs among Arctic stakeholders (Ridley et al. 2016). Nonethe-
112 less, navigation through the Arctic has already increased in frequency as a result of this decline
113 (Melia 2016; Eguíluz et al. 2016) with a substantial opening of trade routes associated with the
114 increased ice-free season by the end of the 21st century (Aksenov et al. 2015; Stephenson and
115 Smith 2013).
116

117 As sea ice reduces in extent, multi-year ice is being lost and there is consequently a larger
118 proportion of seasonal, thin first-year ice (Maykut 1978; Holland et al. 2006). Increased thin ice
119 may result in an ice pack that exhibits greater inter-annual variability (Maslanik et al. 2007b;
120 Goosse et al. 2009; Notz 2009; Kay et al. 2011; Holland and Stroeve 2011; Döscher and Koenigk
121 2013), at least partially due to enhanced ice growth and retreat rates (Maykut 1978; Holland et al.
122 2006; Bathiany et al. 2016a). Decreased ice thickness promotes amplification of a positive ice-
123 albedo feedback, which can magnify sea ice anomalies (Perovich et al. 2007), and thin ice is
124 more vulnerable to anomalous atmospheric forcing and oceanic transport due to the smaller
125 amount of energy required to completely melt the ice (Maslanik et al. 1996, Zhao et al. 2018).
126 For example, pulse-like increases in oceanic heat transport can trigger abrupt ice-loss events in
127 sufficiently thin ice (Woodgate et al. 2012).
128

129 The relationship between ice area and its variability has been studied in a limited capac-
130 ity, likely because it is only beginning to become visible in September in the present day. Both
131 Goosse et al. (2009) and Swart et al. (2015; their Fig. S6) reported that maximum sea ice varia-
132 bility during September occurs once the mean ice extent declines to 3-4 million km². This in-
133 creased variability may occur due to increased prevalence of RILEs and periods of rapid recov-
134 ery during this timeframe (Döscher and Koenigk 2013). The thickness distribution during these
135 periods skews toward thinner ice, which is conducive to both rapid ice loss and rapid recovery



136 processes (Tietsche et al. 2011; Döscher and Koenigk 2013). Holland et al. (2008) considered a
137 critical ice thickness that can serve as a precursor to RILEs, but found it more likely that intrinsic
138 variability played the primary role in the particular RILEs that were studied.

139

140 Building on these previous studies that have focused primarily on variability at the sum-
141 mer ice minimum, our paper has two novel aspects. First, we analyze variability of sea ice over
142 the course of the year through the 21st century and find very different behavior across seasons.
143 These monthly differences are important, because marine access to the Arctic will likely expand
144 beyond late summer as the ice pack shrinks. Second, we detail how interannual sea ice area vari-
145 ability changes as the ice pack retreats and link enhanced future variability to optimal ice thick-
146 nesses as well as the various thermodynamic and dynamic processes that control ice area varia-
147 bility. We analyze a large 40-member ensemble for our study, which has the advantage of allow-
148 ing us to robustly characterize internal variability. This allows us to test the hypothesis that inter-
149 annual Arctic sea ice cover variability will increase throughout the year in the future as the ice
150 pack diminishes.

151

152

153 **2. Data and Methods**

154

155 Ice thickness, concentration, and area were obtained from simulations of the Community
156 Earth System Model Large Ensemble Project (CESM-LE). Ice concentration refers to the per-
157 centage of a given grid cell that is covered by ice, while ice area in this study refers specifically
158 to this percent coverage multiplied by the area of the grid cell yielding a total Arctic ice-covered
159 area. The CESM-LE was designed to enable an assessment of projected change in the climate
160 system while incorporating a wide range of internal climate variability (Kay et al. 2015). It con-
161 sists of 40 ensemble members simulating the period 1920-2100 under historical and projected
162 (RCP8.5 emissions scenario only) external forcing. The ensemble members are produced by in-
163 troducing a small, random round-off level difference in the initial air temperature field for each
164 member. This then generates a consequent ensemble spread that is purely due to simulated inter-
165 nal climate variability. A full description of the CESM-LE is given in Kay et al. (2015).

166

167 Another data set used in the current study is the model simulations from the Coupled
168 Model Intercomparison Project Phase 5 (CMIP5). Although more than 40 models submitted their
169 simulation results to the Program for Climate Model Diagnosis and Intercomparison (PCMDI),
170 only 12 of them simulated the Arctic sea ice extent within 20-percent error when compared with
171 observations (Wang and Overland, 2012, Wang and Overland 2015). Therefore, we used only
172 these 12 models identified by Wang and Overland (2015) in this study; there are 33 ensemble
173 members from these 12 models in the RCP8.5 emissions scenario. Sea ice area, rather than ice
174 extent, is obtained from these 12 CMIP5 models to be consistent with CESM-LE results.

175

176 One of our primary analysis datasets is the time series of monthly ice variables. The en-
177 semble mean of all statistics is taken after the statistics are calculated for each ensemble member.
178 1-year differences in ice area are calculated for each month separately to remove the confound-
179 ing effect of amplified variability resulting from a downward trend. Finally, a 10-year running
180 standard deviation is applied to the time series of 1-year differences in monthly ice area, centered
181 on a given year. Ten years was chosen to quantify variability over decadal-scale intervals and to



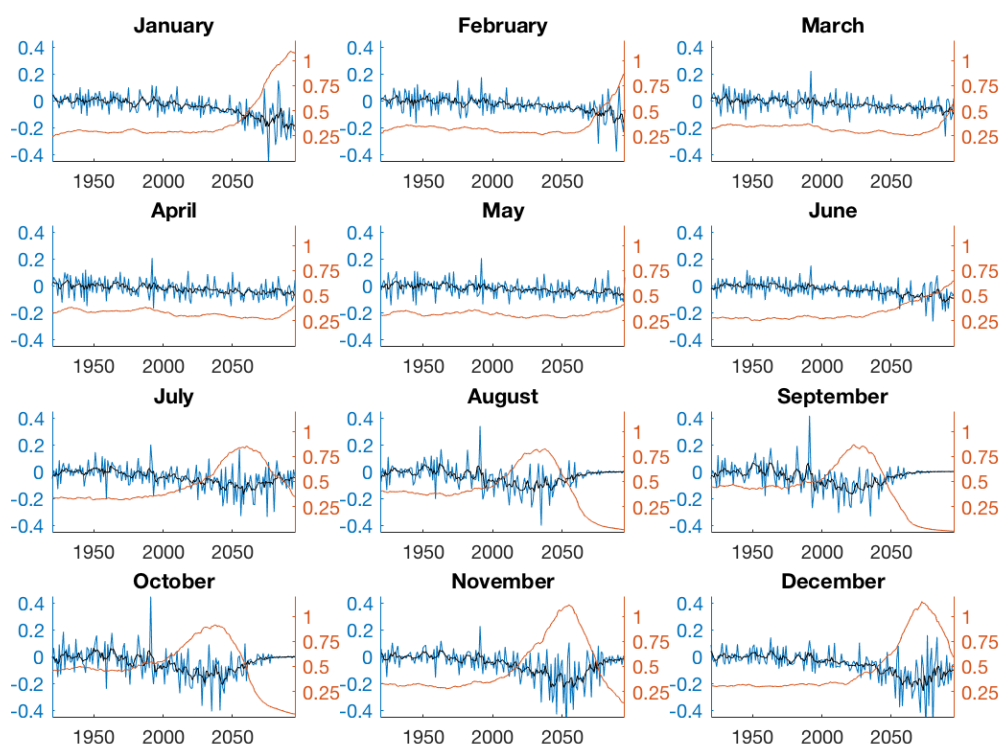
182 provide an adequate number of years for a standard deviation calculation. The timing and magni-
183 tude of variability is generally insensitive to the standard deviation window, however, and
184 whether the 1-year difference in ice area or its raw time series is used.

185
186

187 3. Results

188 3.1 Sea ice area and its variability

189



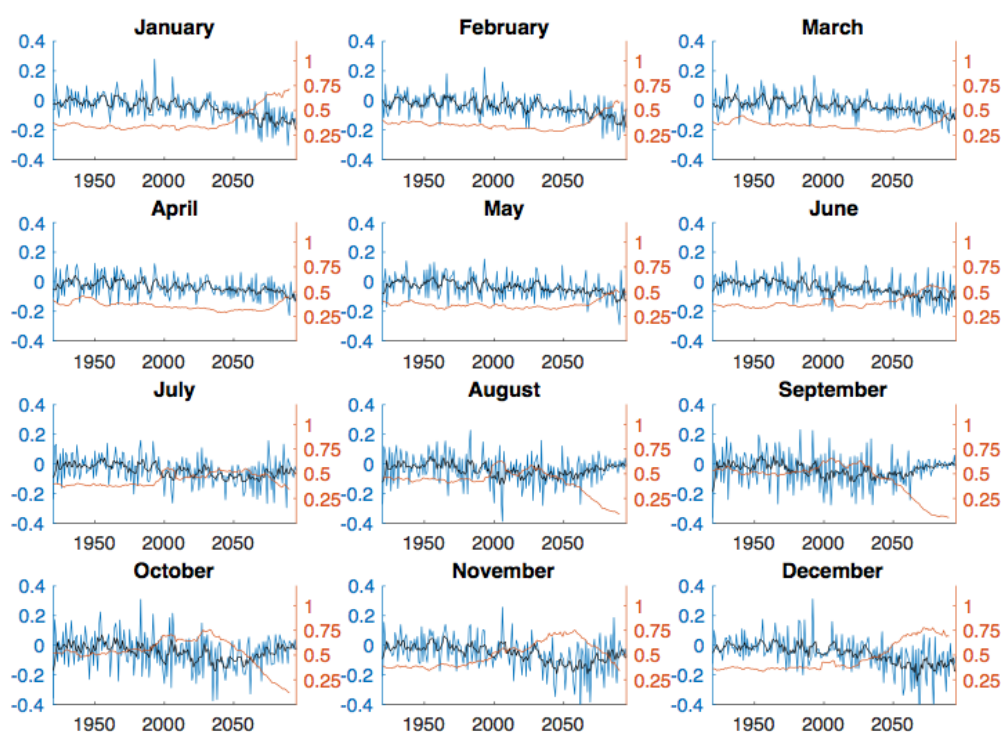
190
191
192
193
194

Figure 1: The CESM-LE ensemble mean of the 1-year differences in sea ice area (blue; $\text{km}^2 \times 10^6$) with their 5-year running mean overlaid (black) and the running standard deviation of the interannual change in sea ice area (gold; $\text{km}^2 \times 10^6$).

195 Sea ice area in the CESM-LE is projected to decline in all months in the 21st century, pro-
196 ceeding in three phases: a fairly stable regime of extensive coverage in the 20th century, then a
197 decline, followed by virtually no ice remaining in summer and autumn months (Fig. S1). Sea ice
198 area variability also follows this three-phase progression in months spanning mid-summer to
199 early winter (Fig. 1). For example, in September this includes a period of modest variability dur-
200 ing the 20th century, then a distinct variability peak in the late 2020s and 2030s that coincides
201 with the maximum rate of ice retreat, and finally negligible variability in the late 21st century as
202 the Arctic reaches near ice-free conditions (Fig. 1). The first two phases of this progression in



203 variability occur for months in late winter to early summer (January-June), and suppressed varia-
204 bility would likely emerge beyond the end of the century, assuming that ice cover in these
205 months would continue to retreat. The maximum rate of ice retreat (negative values of the deriv-
206 ative) occurs at a different time in the 21st century in each month, occurring presently in Septem-
207 ber but not until the end of the century in spring.
208



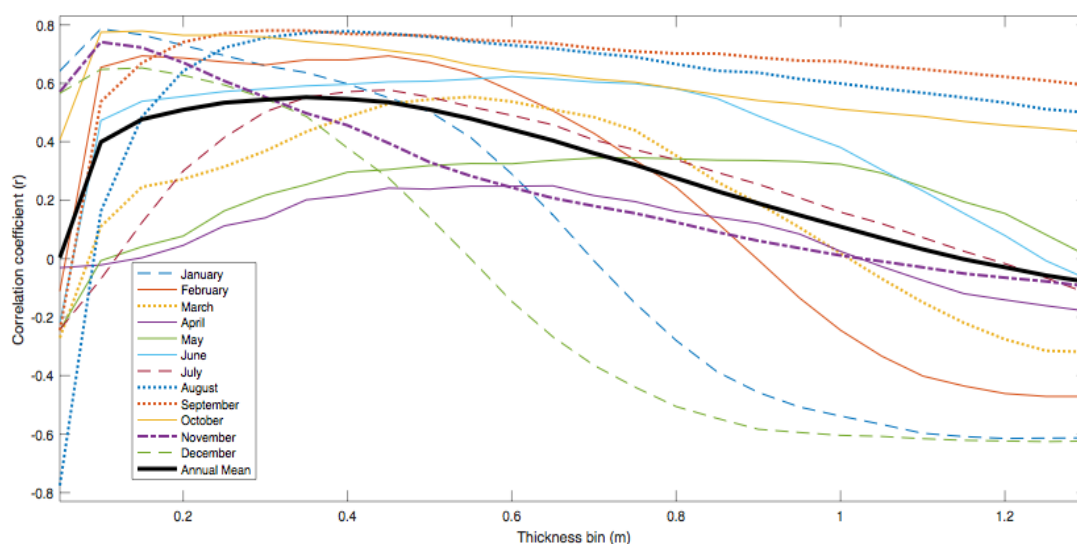
209
210 **Figure 2:** As in Fig. 1, but for the ensemble mean from 12 CMIP5 models' sea ice area.
211

212 The same inverse relationship between ice area and its variability is maintained across
213 CMIP5 models, though with more noise resulting from the aggregation of many different models
214 rather than ensemble members from a single model (Fig. 2). This is most notable in the sea ice
215 area (1-year difference) time series (Fig. 2, blue), indicating that there is considerable spread in
216 when and how the downward trend proceeds each month as found in Massonnet et al. (2012), but
217 good agreement that variability increases in this timeframe.
218

219 The analysis of ice area variability in Fig. 1 and Fig. 2 follows that of Goosse et al.
220 (2009) and Swart et al. (2015), but we extend their findings for September to all months and con-
221 firm that the variability in ice area is maximized as its total basin area decline is well underway
222 in both CESM-LE ensembles and across CMIP5 models. An inverse relationship between the
223 rate of sea ice retreat and the magnitude of variability is present across all months in CESM-LE
224 and CMIP5: the standard deviation is highest when ice declines the fastest (Figs. 1 and 2). Fur-



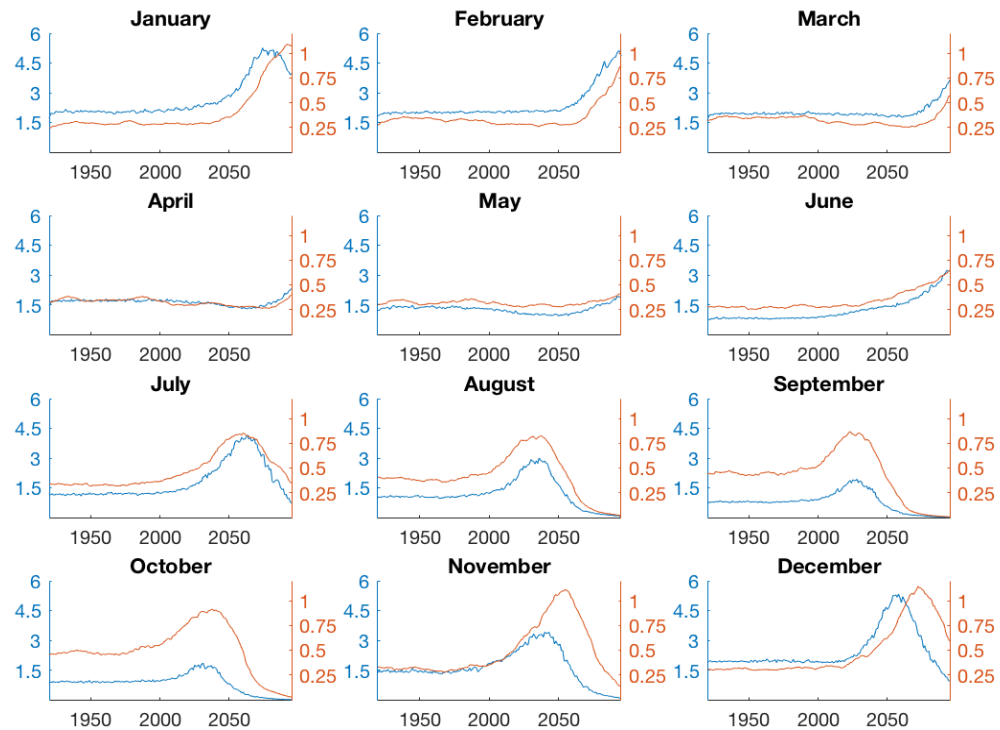
225 furthermore, the magnitude and timing of peak ice area variability in both sets of experiments dif-
226 fers greatly by season. The peak in magnitude in CESM-LE is most pronounced from Novem-
227 ber-January when the running standard deviation of ice area exceeds 1×10^6 km², while the low-
228 est magnitudes occur in April and May, when the downward trend in ice area does not peak prior
229 to 2100 (Fig. 1). Near the end of the 21st century, the running standard deviation also shows an
230 increase in the CMIP5 ensembles from December to June (Fig. 2). Part of this increase is associ-
231 ated with decreasing sea ice cover, but the CMIP5 model spread could also be responsible for in-
232 flated variance as models diverge in their timing of the downward trend and its rate of decline.



233 **Figure 3:** Monthly correlation coefficient (r) of the 2000-2100 10-year running standard devia-
234 tion of 1-year difference in sea ice area with mean grid cell ice thickness binned every 0.05 m of
235 thickness.

237 3.2 Relationship between ice area variability and thickness

238
239 Because increasing future concentrations of thin ice are likely a primary factor in in-
240 creased ice area variability, we next consider the relationship between ice thickness and its varia-
241 bility in CESM-LE. This is done by correlating the standard deviation of basin-wide ice area
242 (Fig. 1) with the total area of grid cells with mean ice thickness within a given range for an ag-
243 gregation of all years and ensemble members, binned at 0.05 m intervals (Fig. 3). 20th century
244 data are omitted because both variables are largely stationary for this period. There is a large dif-
245 ference in the maximum correlation coefficient across seasons, but in most months it peaks be-
246 tween $r = 0.6$ and $r = 0.8$. This peak is associated with the thinnest ice of 0.1 m to 0.2 m from
247 October to January. There is a broad peak in the correlation coefficient between 0.25 m and 0.40
248 m in August and September, while July peaks near 0.45 m thickness but with a weaker maximum
249 correlation coefficient ($r = 0.6$). In June, $r = 0.6$ for most ice thicknesses below 0.8 m, and there
250 is only a weak correlation between these variables in April and May.

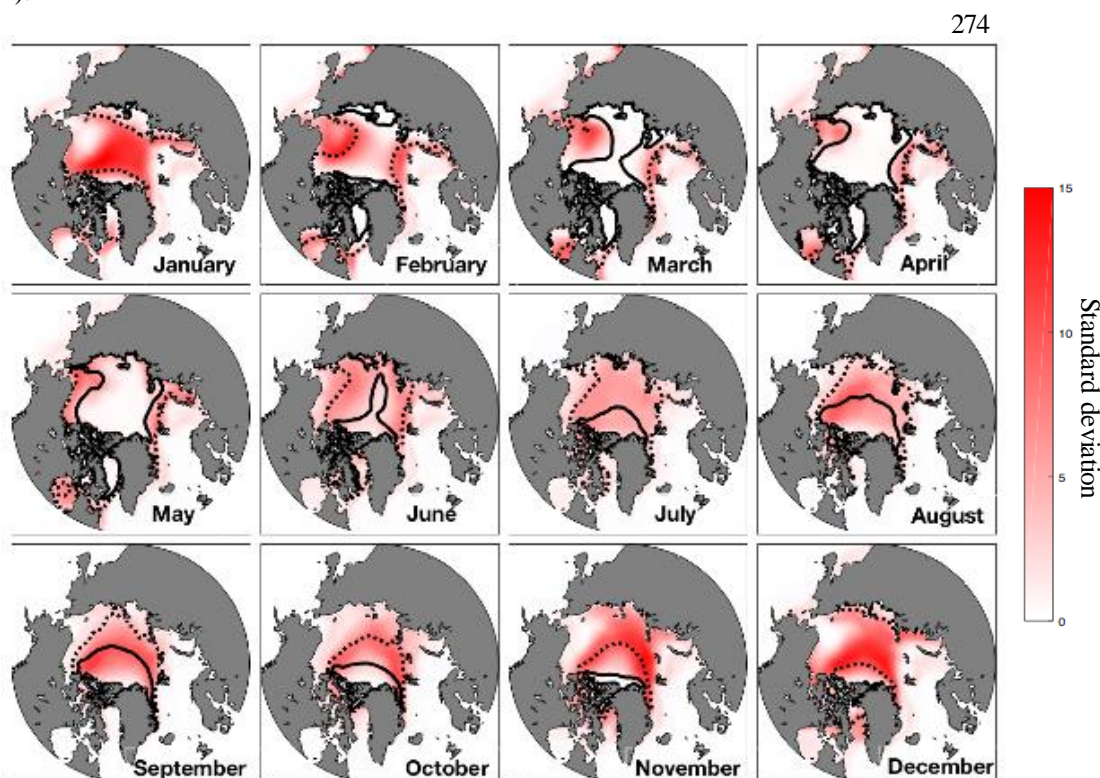


251
 252 **Figure 4:** The CESM-LE ensemble mean of the 10-year running standard deviation of 1-year
 253 difference in sea ice area from Figure 1 (gold; $\text{km}^2 \times 10^6$) and the ensemble mean total area of
 254 grid cells with mean ice thickness between 0.2 m and 0.6 m (blue; $\text{km}^2 \times 10^6$).
 255

256 The analysis in Fig. 3 allows us to identify a common range of ice thicknesses when ice
 257 area variability generally peaks regardless of the month, which we approximate as 0.2 m to 0.6
 258 m. We next track the temporal evolution of this thin ice throughout the basin by calculating the
 259 total area of ice that falls within that range. The time-transgressive nature of when the peak in
 260 thin ice cover occurs (earliest in September, latest in winter-spring) is consistent with the corre-
 261 sponding timing of the peak future sea ice area variability, suggesting that the emergence of a
 262 sufficiently thin and contracted ice pack is a primary factor for enhanced ice cover variability
 263 (Fig. 4). Both curves match each other in shape, with a steady state early, increasing to a peak
 264 and dropping to zero as the Arctic becomes ice-free. The exception is in the spring and early
 265 summer when neither increases until the end of the 21st century, when ice begins to decline more
 266 rapidly. The two curves are largely in phase as well, with one preceding the other by no more
 267 than 10-20 years in July, August, and November–January. The phase difference is due to the
 268 chosen range of ice thicknesses, since the best relationship varies by month (Fig. 3). The two
 269 curves are in phase from August–October (Fig. 4) when the 0.2 m to 0.6 m range approximates
 270 the best relationship between thickness and variability (Fig. 3). However, ice area variability



271 maximizes after the peak in 0.2 m – 0.6 m thickness area in November–January, because varia-
272 bility is more highly correlated with ice slightly thinner than 0.2 m in these months (Fig. 3; Fig.
273 4).



275 **Figure 5:** Monthly ensemble average of the 10-year running standard deviation of ice concentra-
276 tion (%) in the decade when ice area variability is maximum. Mean 0.2 m and 0.6 m ice thick-
277 nesses are indicated by the dotted and solid contours, respectively.

278
279 There are also notable seasonal differences in the spatial pattern of variability during the
280 decade when variability in ice concentration peaks in CESM-LE (Fig. 5). The largest fluctuations
281 occur in a horseshoe-shaped pattern across the Arctic Ocean in autumn, but they are restricted to
282 the boundaries of the Atlantic and Pacific Oceans in late winter and spring. The result is a larger
283 area of high variability in the second half of the year and into January. The mean 0.2 m (dotted)
284 and 0.6 m (solid) ice thickness contours are overlaid for reference (Fig. 5). The contours corre-
285 spond closely to the boundary of maximum variability in ice coverage in most months, which is
286 consistent with results from Fig. 3 and Fig. 4. This demonstrates the first-order relationship be-
287 tween thin ice and inter-annual ice coverage within a given region.

289 3.3 Ice concentration tendency

290



291 The strong relationship between thin ice coverage and high concentration variability oc-
292 curs primarily due to the differing underlying mechanisms controlling ice concentration variabil-
293 ity at a given time, namely whether ice is growing or retreating. To illustrate this, we chose two
294 months representative of these processes, September and December, to conduct an in-depth anal-
295 ysis of the physical mechanisms involved in the time difference in the two curves in Fig. 4. Sep-
296 tember is the end of the melt season, and therefore the ice concentration over the entire basin in
297 this month reflects the cumulative impact of melt processes throughout the summer. By contrast,
298 December is a time of ice growth, particularly in the future, and thus the ice concentration in this
299 month is largely regulated by cumulative growth processes during the autumn. Using available
300 model output, we calculate the ice concentration tendency ($\% \text{ day}^{-1}$) from thermodynamics and
301 dynamics in the regions where the decadal standard deviation of ice concentration exceeds 30%
302 within the grid cell (Fig. S2) to evaluate the mean ice budget. These regions of maximum varia-
303 bility in September and December closely match those in Fig. 5, though the magnitude is smaller
304 in Fig. 5 due to a slightly different method of calculating the standard deviation. The daily
305 change in ice concentration is a function of dynamic contributions (ice import/export and ridg-
306 ing), thermodynamic melt processes (top, basal, and lateral), and thermodynamic growth (frazil
307 and congelation). Because antecedent conditions of the icepack can be an important factor for
308 determining ice concentration in the month of interest, we sum these terms over the preceding
309 months (July-September or October-December) and report the net 3-month change in ice concen-
310 tration resulting from each component.

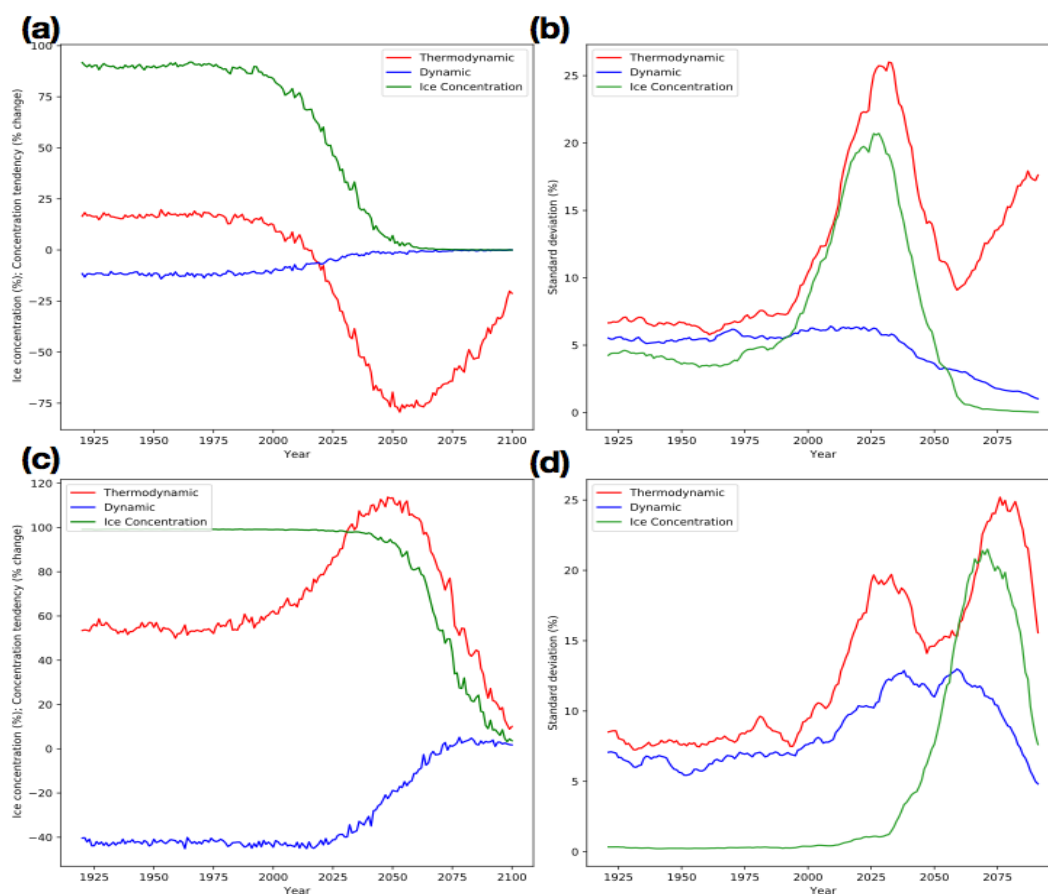
311
312 The most interannually variable ice cover during September occurs primarily in the 2020s
313 and is centered across the central Arctic (Fig. S2a), though this region displays net ice expansion
314 in July-September in the 20th century (Fig. 6a) due to rapid ice growth in September. Thermody-
315 namic processes dominate over dynamics and are of opposing sign during the 20th century, and
316 thermodynamic processes add an average of 20% to the ice concentration of each grid cell in the
317 region by the end of September, compared with a loss of only 10% from dynamical processes
318 (Fig. 6a). Ice growth diminishes and melt processes accelerate in the early-mid 21st century
319 when the melt processes reduce ice concentration by more than 75% and the dynamic processes
320 essentially disappear with less ice to export (Fig. 6a). After 2060, September ice free conditions
321 occur, and the thermodynamic term becomes less negative due to reduced areal coverage of ice
322 in June and hence less ice area to melt over the summer (Fig. 6a).

323
324 Because thermodynamic processes dominate in controlling ice concentration in the fu-
325 ture, they should also be the first-order forcing explaining future ice concentration variability,
326 particularly given that the magnitude of the dynamic contribution approaches zero by the 2020s
327 when ice cover is rapidly diminishing. As shown in Figure 6b, the peak interannual variability in
328 the thermodynamic term (red curve) is indeed several times larger than peak variability of the
329 dynamic term (blue curve), and the thermodynamic variability maximizes during the late 2020s
330 in phase with the variability of the ice concentration (green curve) when the thermodynamic term
331 is declining most rapidly in Figure 6a. The thermodynamic term variability likely also reflects
332 the influence of the surface albedo feedback in amplifying summer ice area variations as well.
333 There is a secondary rise in the variability of the thermodynamic term after 2060 (Figure 6b), co-
334 inciding with its rapid rise toward zero in Figure 6a, but ice coverage by this point is confined to
335 a diminishing area.

336



337 Ice growth rather than melt occurs in the October-December period in a similar region of
 338 maximum interannual variability as September, except slightly equatorward (Fig. S2b), from the
 339 20th century well into the 21st century, and ice export plays a relatively larger role in the regions
 340 of interest in December than in September (Fig. 6c). However, the thermodynamic tendency is
 341 still the dominant term controlling ice concentration within this region of maximum interannual
 342 variability, and this term increases in the early 21st century to a total of nearly 120%, some of
 343 which is offset by ice export that contributes to a 40% decrease in mean ice concentration in the
 344 20th and early 21st centuries (Fig. 6c). The increased net ice growth occurs at this time primarily
 345 because there is more initial open water on which frazil can form.
 346
 347



348
 349 **Figure 6:** Time series of ensemble-mean a) September ice concentration (%) and July-Septem-
 350 ber averaged concentration tendency (% day⁻¹) from dynamics and thermodynamics, and b) the
 351 10-year running standard deviation of: the inter-annual difference in ice concentration (%), and



352 July–September ice concentration tendency from dynamics and thermodynamics (% day⁻¹). The
353 same information is presented in c) and d) for December concentration and October–December
354 ice concentration tendency terms.

355
356 Figure 6d shows that the standard deviation of December ice concentration (green curve)
357 peaks around 2070 and is accompanied by a peak in the variability of the thermodynamic ten-
358 dency (red curve) of more than double the magnitude of its dynamic tendency (blue curve). A
359 smaller first peak in thermodynamic tendency occurs in the 2020s, when ice growth in this re-
360 gion increases due to increased frazil growth as this region’s waters become more open on aver-
361 age in October. This initial peak may be smaller due to the anti-correlation between dynamic and
362 thermodynamic tendency which reduces the effect of the latter. The rapid subsequent decline in
363 ice growth occurs as conditions become too warm for ice growth over much of the October–De-
364 cember period in the 2050s and 2060s (Fig. 6c). This is reflected in the peak in variability of the
365 thermodynamic tendency (red curve) approximately corresponding to the timing of the peak in
366 the ice area variability (green curve) in 2070 (Fig. 6d). The coincidence in their peak variability
367 is similar to that in Figure 6b and underscores the dominance of thermodynamics over dynamics
368 in regulating the variability of ice area.

369
370

371 **4. Discussion and Conclusions**

372

373 1) Inter-annual variability of Arctic sea ice cover increases in all months in the future as sea
374 ice area and thickness decline, but there is a strong seasonal dependence. There is also a strong
375 seasonal dependence of the magnitude of the maximum ice area variability in the future, with the
376 greatest magnitude occurring during autumn and winter and smallest during spring (Fig. 1,2).
377 The future peak in variability emerges soonest in late-summer months and latest during spring
378 months, and the magnitude of this peak is inversely correlated with the rate of ice loss in every
379 month.

380

381 It is possible that the seasonal differences in ice area variability are partially a construction
382 of the geography of the Arctic Basin, as evident in Fig. 5: when the ice margin is geographically
383 constrained and unable to expand and contract due to a coastline early in the simulation, there is
384 a smaller area subject to high ice variability. This explanation was offered by Goosse et al.
385 (2009) for the same relationship in summer ice area variability, as well as by Eisenman (2010) to
386 explain retreat rate differences between summer and winter. However, in the future the ice in the
387 central Arctic Ocean becomes thin enough to expand and contract extensively each season, lead-
388 ing to an increase in variability. Therefore, variability could be considered to be limited particu-
389 larly in the first phase of its time series (Fig. 1) by the inability of ice to spread across a large
390 open area. Furthermore, results from Fig. 3 and Fig. 4 suggest that the amount of thin ice alone
391 can explain the evolution of ice variability in every month, though differences in the optimal ice
392 thickness by month may require a partial geographical explanation in addition to one incorporat-
393 ing the components of the thermodynamic tendency of ice area from Fig. 6.

394

395 2) Ice needs to be sufficiently thin before areal variability maximizes, and in CESM-LE the
396 optimal thickness range is generally between 0.2 m to 0.6 m but with some seasonal dependence
397 resulting from the ice melt or ice growth processes that dominate in a given season (Fig. 3-5).



398 The mean ice thickness in late summer and autumn is close to 0.6 m when ice area variability is
399 highest, but is 0.2 m or less for a grid cell average in the winter.

400

401 Increased ice area variability in summer and fall is partly attributable to a higher effi-
402 ciency of open water formation with the thinning sea ice (Holland et al., 2006) and the fact that
403 smaller heating anomalies are required to completely melt through vast areas of the thin ice pack
404 (Bitz and Roe, 2004). We find that the total area of thin ice between the range 0.2 m to 0.6 m is
405 closely related to how soon and how strongly the peak variability in basin-wide ice area emerges,
406 and this is primarily a function of variability in ice area's thermodynamic tendency. This is con-
407 sistent with a physical understanding of this relationship, since ice that is too thin tends to be sea-
408 sonal and melt off every year, whereas thick ice is more likely to survive the melt season. Sea-
409 sonal forecasting of September sea ice coverage takes advantage of this concept, with the fore-
410 cast skill improved when initializing ice thickness up to 8 months in advance (Chevallier et al.,
411 2012; Day et al., 2014).

412

413 In contrast, ice area variability in November-January arises primarily from inter-annual
414 variability in ice growth (Fig. 6c,d), which is dependent on existing open water conditions and
415 temperature anomalies. The peak in ice area variability also coincides with a slightly lower mean
416 ice thickness of 0.2 m, though it is unclear whether that is due to these ice growth rather than
417 melt processes at work during the winter.

418

419 3) Interannual variability in ice concentration is driven primarily by thermodynamic mecha-
420 nisms, which are primarily comprised of either ice growth or ice melt depending on the season.
421 Despite being opposing processes, they both exceed in magnitude that of dynamic ice processes
422 (Fig. 6).

423

424 The thermodynamic tendency in ice concentration is of much greater magnitude than its
425 dynamic counterpart at both the end of the melt season and start of the growth season, and the
426 maximum interannual variability of the thermodynamic term is mostly in phase with that of ice
427 concentration. The inverse relationship between ice area's interannual variability and its interan-
428 nual rate of change (Figs. 1 and 2) is also found between the thermodynamic tendency and its
429 rate of change (not shown, but inferred from Fig. 6). This is further evidence that ice area varia-
430 bility is primarily driven by thermodynamic processes in the icepack.

431

432 The dominance of the thermodynamic tendency is unsurprising and has been established as
433 the relatively more important set of processes controlling sea ice variability, primarily via
434 transport of mid-latitude eddy heat flux anomalies (Kelleher and Screen, 2018), anticyclone pas-
435 sage (Wernli and Lukas, 2018), and increased ocean heat transport (Li et al., 2018). However,
436 the dynamic contribution to changes in ice concentration can likely be substantial in the absence
437 of regional and monthly averaging, and numerous mechanisms have been described that can gen-
438 erate increased ice transport. Recent examples include divergent ice drift events connected to
439 anomalous circulation patterns (Zhao et al., 2018) as well as the collapse of the Beaufort High
440 (Petty, 2018; Moore et al., 2018), both of which may become more common in the future due to
441 preconditioning of the icepack and further intrusion of mid-latitude cyclones into the Arctic.

442



443 This study offers a unique contribution by focusing on the predicted evolution of Arctic
444 sea ice variability throughout the year, as characterized by its response to external greenhouse
445 forcing superimposed on short-term internal variability. Increased inter-annual variability in the
446 CESM Large Ensemble as sea ice declines most rapidly is an important result that needs to be
447 accounted for as the ice-free season expands and the timing of maximum variability shifts from
448 September. We also confirm that this relationship is maintained across CMIP5 models, suggest-
449 ing that the responsible mechanisms reported here are robust. These results have important impli-
450 cations for marine navigation going forward, suggesting that the otherwise auspicious transition
451 to diminished sea ice in every month will be accompanied by a confounding increase in inter-an-
452 nual variability of the ice cover before the ice disappears completely.

453

454

455

456 Acknowledgements

457

458 Support was provided by the NOAA Climate Program Office under Climate Variability and Pre-
459 dictability Program grant NA15OAR4310166. This project is partially funded by the Joint Insti-
460 tute for the Study of the Atmosphere and Ocean (JISAO) under NOAA Cooperative Agreement
461 NA10OAR4320148, contribution number 2017-087, the Pacific Marine Environmental Labora-
462 tory contribution number 4671. We would like to acknowledge high-performance computing
463 support from Yellowstone ([ark:/85065/d7wd3xhc](https://doi.org/10.7927/H4T3-9Q95)) provided by NCAR's Computational and In-
464 formation Systems Laboratory, sponsored by the National Science Foundation.

465

466

467

468

469 References

470

- 471 Aksenov, Y., E. E. Popova, A. Yool, A. J. G. Nurser, T. D. Williams, L. Bertino, and J. Bergh:
472 On the future navigability of Arctic sea routes: High-resolution projections of the Arctic
473 Ocean and sea ice, *Mar. Policy*, 1–18, doi:10.1016/j.marpol.2015.12.027, 2015.
- 474 Bathiany, S., B. van der Bolt, M. S. Williamson, T. M. Lenton, M. Scheffer, E. H. van Nes, and
475 D. Notz: Statistical indicators of Arctic sea-ice stability – prospects and limitations,
476 *Cryosph.*, 10(4), 1631–1645, doi:10.5194/tc-10-1631-2016, 2016.
- 477 Bitz, C. M., and G. H. Roe: A mechanism for the high rate of sea ice thinning in the Arctic
478 Ocean, *J. Clim.*, 17(18), 3623–3632, doi:10.1175/1520-0442(2004)017, 2004.
- 479 Cavalieri, D. J., and C. L. Parkinson: Arctic sea ice variability and trends, 1979–2010, *Cryosph.*,
480 6(4), 881–889, doi:10.5194/tc-6-881-2012, 2012.
- 481 Collins, M. et al.: Long-term Climate Change: Projections, Commitments and Irreversibility.
482 Intergovernmental Panel on Climate Change, 108, 2013.
- 483 Comiso, J. C., W. N. Meier, and R. Gersten: Variability and trends in the Arctic Sea ice cover:
484 Results from different techniques, *J. Geophys. Res. Ocean.*, 122, 1–22,
485 doi:10.1002/2017JC012768.
- 486 Ding, Q., et al., Influence of high-latitude atmospheric circulation changes on summertime
487 Arctic sea ice, *Nat. Clim. Chang.*, 7, 289–295, doi:10.1038/nclimate3241, 2017.



- 488 Döscher, R., and T. Koenigk: Arctic rapid sea ice loss events in regional coupled climate
489 scenario experiments, *Ocean Sci. Discuss.*, 9(4), 2327–2373, doi:10.5194/osd-9-2327-
490 2012, 2012.
- 491 Goosse, H., O. Arzel, C.M. Bitz, A. de Montety, and M. Vancoppenolle: Increased variability of
492 the Arctic summer ice extent in a warmer climate, *Geophys. Res. Lett.*, 36, L23702,
493 doi :10.1029/2009GL040546, 2009.
- 494 Holland, M. M., C. M. Bitz, and B. Tremblay: Future abrupt reductions in the summer Arctic sea
495 ice, *Geophys. Res. Lett.*, 33(23), 1–5, doi:10.1029/2006GL028024, 2006.
- 496 Holland, M. M., C. M. Bitz, L. B. Tremblay, and D. A. Bailey: The role of natural versus forced
497 change in future rapid summer Arctic ice loss. Arctic sea ice decline: Observations,
498 projections, mechanisms, and implications, E.T. DeWeaver, C.M. Bitz, and L.B.
499 Tremblay, Eds., *Geophysical Monograph Series*, American Geophysical Union,
500 Washington, 133-150 doi:10.1029/180GM10, 2008.
- 501 Holland, M. M., and J. Stroeve: Changing seasonal sea ice predictor relationships in a changing
502 Arctic climate, *Geophys. Res. Lett.*, 38, L18501, doi:10.1029/2011GL049303, 2011.
- 503 Jahn, A., J. E. Kay, M. M. Holland, and D. M. Hall: How predictable is the timing of a summer
504 ice-free Arctic?, *Geophys. Res. Lett.*, 1–8, doi:10.1002/2016GL070067, 2016.
- 505 Eguíluz, V. M., J. Fernández-Gracia, X. Irigoien, and C. M. Duarte: A quantitative assessment of
506 Arctic shipping in 2010–2014, *Sci. Rep.*, 6(August), 30682, doi:10.1038/srep30682,
507 2016.
- 508 Eisenman, I.: Geographic muting of changes in the Arctic sea ice cover, *Geophys. Res. Lett.*,
509 37(16), doi:10.1029/2010GL043741, 2010.
- 510 Kay, J. E. et al.: The Community Earth System Model (CESM) Large Ensemble Project: A
511 Community Resource for Studying Climate Change in the Presence of Internal Climate
512 Variability, *Bull. Am. Meteorol. Soc.*, 96(8), 1333–1349, doi:10.1175/BAMS-D-13-
513 00255.1, 2015.
- 514 Kay, J. E., M. M. Holland, and A. Jahn: Inter-annual to multi-decadal Arctic sea ice extent trends
515 in a warming world. *Geophys. Res. Lett.*, 38, L15708, doi:10.1029/2011GL048008,
516 2011.
- 517 Kelleher, M., and J. Screen: Atmospheric precursors of and response to anomalous Arctic sea ice
518 in CMIP5 models, *Adv. Atmos. Sci.*, 35(27), doi.org/10.1007/s00376-017-7039-9.
- 519 Khon, V. C., I. I. Mokhov, M. Latif, V. A. Semenov, and W. Park: Perspectives of Northern Sea
520 Route and Northwest Passage in the twenty-first century, *Clim. Change*, 100(3), 757–
521 768, doi:10.1007/s10584-009-9683-2, 2010.
- 522 Kwok, R., and D. A. Rothrock: Decline in Arctic sea ice thickness from submarine and ICESat
523 records: 1958–2008, *Geophys. Res. Lett.*, 36(15), doi:10.1029/2009GL039035.
- 524 Kwok, R., G. F. Cunningham, M. Wensnahan, I. Rigor, H. J. Zwally, and D. Yi: Thinning and
525 volume loss of the Arctic Ocean sea ice cover: 2003–2008, *J. Geophys. Res. Ocean.*,
526 114(7), 2003–2008, doi:10.1029/2009JC005312, 2009.
- 527 Labe, Z., Magnusdottir, G., and H. Stern: Variability of Arctic Sea Ice Thickness Using
528 PIOMAS and the CESM Large Ensemble, *J. Climate*, 31, 3233–3247,
529 [DOI.ORG/10.1175/JCLI-D-17-0436.1](https://doi.org/10.1175/JCLI-D-17-0436.1), 2018.
- 530 Lang, A., S. Yang, and E. Kaas: Sea ice thickness and recent Arctic warming, *Geophys. Res.*
531 *Lett.*, 44, doi:10.1002/2016GL071274, 2017.



- 532 Li, D., R. Zhang, and T. Knutson: Comparison of Mechanisms for Low-Frequency Variability of
533 Summer Arctic Sea Ice in Three Coupled Models, *J. Climate*, 31, 1205–
534 1226, [DOI.ORG/10.1175/JCLI-D-16-0617.1](https://doi.org/10.1175/JCLI-D-16-0617.1), 2018.
- 535 Maslanik, J. A., M. C. Serreze, and R. G. Barry: Recent decreases in Arctic summer ice cover
536 and linkages to atmospheric circulation anomalies, *Geophys. Res. Lett.*, 23(13), 1677–
537 1680, doi:10.1029/96GL01426, 1996.
- 538 Maslanik, J., S. Drobot, C. Fowler, W. Emery, and R. Barry: On the Arctic climate paradox and
539 the continuing role of atmospheric circulation in affecting sea ice conditions, *Geophys.*
540 *Res. Lett.*, 34(3), 2–5, doi:10.1029/2006GL028269, 2007a.
- 541 Maslanik, J. A., C. Fowler, J. Stroeve, S. Drobot, J. Zwally, D. Yi, and W. Emery: A younger,
542 thinner Arctic ice cover: Increased potential for rapid, extensive sea-ice loss, *Geophys.*
543 *Res. Lett.*, 34(24), 2004–2008, doi:10.1029/2007GL032043, 2007b.
- 544 Maslanik, J., J. Stroeve, C. Fowler, and W. Emery: Distribution and trends in Arctic sea ice age
545 through spring 2011, *Geophys. Res. Lett.*, 38(13), 2–7, doi:10.1029/2011GL047735,
546 2011.
- 547 Massonnet, F., T. Fichefet, H. Goosse, C. M. Bitz, G. Philippon-Berthier, M. M. Holland, and P.
548 Y. Barriat: Constraining projections of summer Arctic sea ice, *Cryosphere*, 6(6), 1383–
549 1394, doi:10.5194/tc-6-1383-2012, 2012.
- 550 Maykut, G. A.: Energy exchange over young sea ice in the central Arctic, *J. Geophys. Res.*,
551 83(C7), 3646, doi:10.1029/JC083iC07p03646, 1978.
- 552 Melia, N., K. Haines, and E. Hawkins: Sea ice decline and 21st century trans-Arctic shipping
553 routes, *Geophys. Res. Lett.*, 43(18), 9720–9728, doi:10.1002/2016GL069315, 2016.
- 554 Moore, G. W. K., Schweiger, A., Zhang, J., and M. Steele: Collapse of the 2017 winter Beaufort
555 High: A response to thinning sea ice? *Geophysical Research Letters*, 45, 2860–2869,
556 doi.org/10.1002/2017GL076446, 2018
- 557 Nghiem, S. V., I. G. Rigor, D. K. Perovich, P. Clemente-Colón, J. W. Weatherly, and G. Neu-
558 mann: Rapid reduction of Arctic perennial sea ice, *Geophys. Res. Lett.*, 34(19), 1–6,
559 doi:10.1029/2007GL031138, 2007.
- 560 Notz, D.: The future of ice sheets and sea ice: between reversible retreat and unstoppable loss.,
561 *Proc. Natl. Acad. Sci. U. S. A.*, 106(49), 20590–5, doi:10.1073/pnas.0902356106, 2009.
- 562 Notz, D., and J. Marotzke: Observations reveal external driver for Arctic sea-ice retreat,
563 *Geophys. Res. Lett.*, 39(8), 1–6, doi:10.1029/2012GL051094, 2012.
- 564 Notz, D., and J. Stroeve: Observed Arctic sea-ice loss directly follows anthropogenic CO₂
565 emission, *Science*, 354(6313), 747–750, doi:10.1126/science.aag2345, 2016.
- 566 Overland, J. E., and M. Wang: When will the summer Arctic be nearly sea ice free?, *Geophys.*
567 *Res. Lett.*, 40(10), 2097–2101, doi:10.1002/grl.50316, 2013.
- 568 Perovich, D. K., B. Light, H. Eicken, K. F. Jones, K. Runciman, and S. V. Nghiem: Increasing
569 solar heating of the Arctic Ocean and adjacent seas, 1979–2005: Attribution and role in
570 the ice-albedo feedback, *Geophys. Res. Lett.*, 34(19), 1–5, doi:10.1029/2007GL031480,
571 2007.
- 572 Petty, A. A.: A possible link between winter Arctic sea ice decline and a collapse of the Beaufort
573 High? *Geophysical Research Letters*, 45, 2879–2882,
574 [DOI.ORG/10.1002/2018GL077704](https://doi.org/10.1002/2018GL077704), 2018.
- 575 Ridley, J. K., R. A. Wood, A. B. Keen, E. Blockley, and J. A. Lowe: Brief Communication:
576 Does it matter exactly when the Arctic will become ice-free?, *Cryosph. Discuss.*,
577 (March), 1–4, doi:10.5194/tc-2016-28, 2016.



- 578 Serreze, M. C., and J. C. Stroeve: Arctic sea ice trends, variability and implications for seasonal
579 ice forecasting, *Philos. Trans. R. Soc. A Math. Phys. Eng. Sci.*, 373(2045), 20140159,
580 doi:10.1098/rsta.2014.0159, 2015.
- 581 Stephenson, S. R., L. C. Smith, L. W. Brigham, and J. A. Agnew: Projected 21st-century
582 changes to Arctic marine access, *Clim. Change*, 118(3–4), 885–899, doi:10.1007/s10584-
583 012-0685-0, 2013.
- 584 Stammerjohn, S., R. Massom, D. Rind, and D. Martinson: Regions of rapid sea ice change: An
585 inter-hemispheric seasonal comparison, *Geophys. Res. Lett.*, 39(6), L06501,
586 doi:10.1029/2012GL050874, 2012.
- 587 Stroeve, J. C., M. C. Serreze, M. M. Holland, J. E. Kay, J. Malanik, and A. P. Barrett: The
588 Arctic's rapidly shrinking sea ice cover: a research synthesis, *Clim. Change*, 110(3–4),
589 1005–1027, doi:10.1007/s10584-011-0101-1, 2012.
- 590 Stroeve, J., M. M. Holland, W. Meier, T. Scambos, and M. Serreze: Arctic sea ice decline: Faster
591 than forecast, *Geophys. Res. Lett.*, 34(9), 1–5, doi:10.1029/2007GL029703, 2007.
- 592 Swart, N. C., J. C. Fyfe, E. Hawkins, J. E. Kay, and A. Jahn: Influence of internal variability on
593 Arctic sea-ice trends, *Nat. Clim. Chang.*, 5(2), 86–89, doi:10.1038/nclimate2483, 2015.
- 594 Tietsche, S., D. Notz, J. H. Jungclaus, and J. Marotzke: Recovery mechanisms of Arctic summer
595 sea ice, *Geophys. Res. Lett.*, 38(2), 1–4, doi:10.1029/2010GL045698, 2011.
- 596 Wang, M., and J. E. Overland: A sea ice free summer Arctic within 30 years? *Geophys. Res.*
597 *Lett.*, 36, L07502, doi:10.1029/2009GL037820, 2009.
- 598 Wang, M., and J. E. Overland: A sea ice free summer Arctic within 30 years: An update from
599 CMIP5 models, *Geophys. Res. Lett.*, 39(18), doi:10.1029/2012GL052868, 2012.
- 600 Wang, M., and J. E. Overland: Projected future duration of the sea-ice-free season in the Alaskan
601 Arctic, *Prog. Oceanogr.*, 136, 50–59, doi:10.1016/j.pocean.2015.01.001, 2015.
- 602 Wernli, H., and L. Papritz: Role of polar anticyclones and mid-latitude cyclones for Arctic
603 summertime sea-ice melting, *Nat. Geos.*, 11, 108–113, doi:10.1038/s41561-017-0041-0,
604 2018.
- 605 Woodgate, R. A., T. J. Weingartner, and R. Lindsay: Observed increases in Bering Strait oceanic
606 fluxes from the Pacific to the Arctic from 2001 to 2011 and their impacts on the Arctic
607 Ocean water column, *Geophys. Res. Lett.*, 39, L24603, doi:10.1029/2012GL054092,
608 2012.
- 609 Zhao, J., D. Barber, S. Zhang, Q. Yang, X. Wang, and H. Xie: Record Low Sea-Ice
610 Concentration in the Central Arctic during Summer 2010, *Adv. Atmos. Sci.*, 35(January),
611 106–115, doi:10.1007/s00376-017-7066-6, 2018.
- 612
- 613 Zhao, J., D. Barber, S. Zhang, Q. Yang, X. Wang, and H. Xie (2018), Record Low Sea-Ice
614 Concentration in the Central Arctic during Summer 2010, *Adv. Atmos. Sci.*, 35(January),
615 106–115, doi:10.1007/s00376-017-7066-6.
- 616
- 617
- 618
- 619